$\circledS$SAGE

MELK is Upregulated in Advanced Clear Cell Renal Cell Carcinoma and Promotes Disease Progression by Phosphorylating PRAS40

Han Zhang[1] [ORCID]**, Pengtao Wei[1], Wenwei Lv[1], Xingtao Han[1], Jinhui Yang[1], Shuaifeng Qin[1], and Yue Zhang[2]**

Abstract

Clear cell renal cell carcinoma (ccRCC) is the most common type of kidney cancer. However, stage IV ccRCC is generally incurable and its molecular mechanism has not yet been fully clarified. In this study, in order to screen differentially expressed genes (DEGs) between stage IV and stage I ccRCC specimens, we initially analyzed The Cancer Genome Atlas (TCGA) and Gene Expression Omnibus (GSE73731). We found that maternal and embryonic leucine zipper kinase (MELK) is upregulated in stage IV ccRCC samples and that upregulation of MELK is significantly correlated with advanced disease status. Furthermore, both loss and gain-of-function assays strengthen the evidence that MELK enforces the malignant phenotype of ccRCC cells through over-activating the mammalian target of rapamycin complex 1 (mTORC1) pathway. Mechanistically, we verified that the oncogenic effect of MELK occurs through phosphorylating PRAS40, an inhibitory subunit of mTORC1, and through disrupting the interaction between PRAS40 and raptor. In summary, these results elucidate the important role of MELK in the progression of ccRCC and indicate that MELK may be a novel regulator of ccRCC progression by over-activating the mTORC1.

Keywords

differentially expressed genes, clear cell renal cell carcinoma, MELK, mTORC1, PRAS40

Introduction

Renal cell carcinoma (RCC) is the most fatal genitourinary malignancy and about 90% of renal tumors are clear cell renal cell carcinoma (ccRCC)[1]. Compared with stage I ccRCC, stage IV ccRCC is generally incurable and the survival time is shorter. It is thus necessary to study the mechanisms of stage IV ccRCC, and to identify highly specific progression-associated genes for finding new strategies for the treatment of advanced ccRCC. Previous studies have shown that ccRCC is characterized by von Hippel–Lindau (VHL) inactivation[2], a governing event[3] inducing transcription of hypoxia-inducible factors (HIF) target genes, including VEGF, EPO, GLUT-1 and EGFR[4], to accelerate ccRCC progression. Some studies have also reported that HIF-2 is implicated in angiogenesis and ccRCC metastasis[5,6], and obtaining PBRM1 or BAP1 mutation may set the process for ccRCC with different properties[7]. Metastatic ccRCC patients with truncated mutation of the PBRM1 gene gain more clinical benefits from immune checkpoint therapy[8]. Later research has validated that mutations in these genes

were associated with advanced tumor stage[9]. Recently, Ho et al[10]. compared gene expression profiles between patient-matched primary and metastatic RCC tumors and found upregulation of ECM genes in metastases, including SLIT2, ADAMTS12, DCN, LUM, LAMA2, LMO3, and CECAM6. However, the mechanisms and core genes of advanced

[1] Urology Department, Luoyang Central Hospital, Luoyang, Henan, China
[2] Department of Anesthesiology, Tongji Hospital, Tongji Medical College, Huazhong University of Science and Technology, Wuhan, China

Corresponding Authors:
Han Zhang, Luoyang Central Hospital, No. 288, Zhongzhou Road, Luoyang, Henan 471000, China.
Email: hanzhang.henan@mail.com

Yue Zhang, Department of Anesthesiology, Tongji Hospital, Tongji Medical College, Huazhong University of Science and Technology, Jiefang Avenue 1095, 430030, Wuhan, China.
Email: y.zhang0604@hotmail.com

ccRCC need to be further studied and verified. Therefore, the aim of this research is to explore differentially expressed genes (DEGs) through comparing the gene expression profiles of stage I and stage IV ccRCC patients and verify the function and mechanisms of core genes via experiments. First, we conducted bioinformatics analysis for the DEGs and found that maternal embryonic leucine zipper kinase (MELK) is a seed gene in the network module. Then, we tested whether the MELK upregulation could accelerate ccRCC progression through a series of *in vitro* studies where we investigated the function of MELK in tumor cell proliferation, colony formation, migration, and invasion. Mechanistically, MELK could phosphorylate PRAS40 and over-activate mTORC1 by dissociating PRAS40 from raptor, and could subsequently promote the progression of ccRCC. Collectively, these results indicated that MELK may serve as a new therapeutic target in mTORC1 signaling-activated ccRCC cells.

Materials and Methods

Data Collection

The transcriptional data and clinical data of ccRCC are from TCGA (note 1) and GSE73731 (note 2). The RNA sequencing (RNA-seq) data from TCGA included 83 stage IV and 265 stage I ccRCC samples. The RNA-seq data from GSE73731 consisted of 44 stage IV and 41 stage I ccRCC specimens from patients.

Data Pre-processing and DEGs Screening

To screen DEGs, the linear models for microarray data (Limma) package from Bioconductor[11] were adopted to compare stage I and stage IV ccRCC samples from TCGA. Based on the Benjamini and Hochberg method, the associated p-values were adjusted to false discovery rates (FDRs). Q<0.05 and fold change >2 were selected as the cutoff criteria for screening of DEGs. We also used GEO2 R, a web tool applied to screen DEGs by comparing two groups of samples in a GEO series[12], to identify the DEGs between stage I and stage IV ccRCC samples in GSE73731. The adjusted p-value <0.05 and fold change >1.5 were set as the thresholds for identifying DEGs. The online tool Venny2.1 was employed to compare the DEG sets from TCGA and GSE73731 as well as to identify the overlapped DEGs. The genes that appeared in both GSE73731 and TCGA were selected as the final DEGs.

GO and KEGG Pathway Enrichment Analysis of DEGs

Gene ontology (GO) enrichment analysis has been used as functional annotation of large-scale genes. The Database for Annotation, Visualization and Integrated Discovery (DAVID) provides a comprehensive set of functional annotation[13,14]. We carried out GO enrichment and Kyoto Encyclopedia of Genes and Genomes (KEGG) pathway analysis in the DAVID database. The human genome was selected as the research background. A p-value <0.05 and count ≥5 were considered as having significant difference.

PPI Network Construction and Significant Module Extraction

The Search Tool for the Retrieval of Interacting Genes (STRING) database (note 3) offers both experimental and predictive interaction information. It is used for establishing a protein–protein interaction (PPI) network which can help understand the protein function and explain the relationship between proteins on a genome-wide scale[15]. The STRING 10.5 online tool was used to construct the PPI of the DEGs and Cytoscape plugin was used to create network visualization. Further, we analyzed the module of resulting PPI network with the Plugin Molecular Complex Detection (MCODE) with the parameters (node score cutoff ≥2, degree cutoff ≥2, K-core ≥2, and maximum depth =100)[16]. Finally, the seed gene could be identified.

Gene Set Enrichment Analysis

The patients with ccRCC were divided into two groups according to the expression of MELK (median MELK expression value was set as the cutoff). mTORC1 signaling gene set (HALLMARK_MOTRC1_SIGNALING) was obtained from the Molecular Signatures Database from the Broad Institute (note 4). We carried out gene set enrichment analysis by using the default settings, and permutations number was set at 1,000. A p-value <0.05 and FDR <0.25 were considered statistically significant.

Plasmid Construction

pCMV-MELK and pCMV control plasmids were purchased from BioVector (Beijing, China). The lentiviral system with MELK-inducible shRNA transfection starter kit was purchased from SunShineBio (Guangzhou Honsea Sunshine Bio- tech Co., Ltd, China). Catalog #RHS4696-200703132 and cat# RHS4696-200691582 were used for non-template control and shMELK. pENTER-Flag-PRAS40 was purchased from Vigene Biosciences (Shandong, China).

Cell Culture and Transfection

The cell lines ACHN and 769-P were obtained from the American Type Culture Collection (ATCC, Manassas, VA, USA). Cells were cultured in RPMI-1640 medium (Gibco, Carlsbad, CA, USA) supplemented with 10% FBS, at 37°C and 5% CO_2. Cells were transfected with lipofectamine 3000 (Invitrogen, Carlsbad, CA, USA) for plasmid transfection. MELK plasmid and control vector were transfected into 769-P and screened with G418 (700 mg/ml; Amresco, Solon, OH, USA). In addition, shMELK plasmid and shControl vector were transfected into ACHN cell and were screened by using 300 ng/ml puromycin (Sigma, St. Louis, MO, USA).

Cell Proliferation Assay

Cells were cultured in 96-well plates (3,000 cells per well) and incubated for 0–120 h. Viable cells were measured with Cell Counting Kit-8 (Dojindo, Kumamoto, Japan) by using an Enspire, microplate reader (Perkin Elmer, Waltham, MA, USA) at 450 nm.

Cell Colony Formation, Migration, and Invasion Assay

Cells were seeded in six-well plates (300 cells per well) and incubated for 10 days. Then, cells were stained with crystal violet and the colonies (>80 cells) were counted (Becton-Dickinson Biosciences, Bedford, MA, USA). Stable MELK-transfected 769-P, shMELK-1/2#-transfected ACHN, and control cells were cultured at a density of 5×10^5 cells/well in a 6-well plate. The cell monolayer was scratched using a sterile 200 μl pipette tip across the center of the well. The areas of the wound were recorded at 0, 12, and 24 h after culture. Image J analysis software was used to measure the widths of three different wound surfaces within each group. The invasion assay was carried out using modified Boyden chambers coated with matrigel in 24-well plate (Becton-Dickinson Biosciences).

Coimmunoprecipitation

Lysates of 769-P cells transfected with vector, MELK, Flag-PRAS40, and ACHN cells transfected with shNC, shMELK, and Flag-PRAS40 were solubilized, clarified, and incubated with 3 μl anti-Flag antibodies with protein A/G-agarose for 3 h with end-over-end rotation at 4°C. After five washes in 1 ml ice-cold PBS buffer, the immunoprecipitated proteins were eluted from the beads with SDS-PAGE sample buffer.

Western Blot Analysis and Reagent

Cells were lysed in lysis buffer including 0.2% protease inhibitor cocktail III (Calbiochem, San Diego, CA; La Jolla, CA, USA). After homogenization, the cell lysates were incubated on ice for 30 min and centrifuged at 12,000 g for 10 min. The amount of total protein was measured by protein assay kit (Bio-Rad, Hercules, CA, USA), and the proteins were then mixed with SDS sample buffer and boiled for 5 min before loading into a 10% or 8% SDS-PAGE gel (Bio-Rad, Hercules, CA, USA). The proteins were transferred onto nitrocellulose membrane after electrophoresis. The blots were blocked and then incubated with primary antibody followed by a horseradish peroxidase (HRP)-conjugated secondary antibody. Immunoreactive bands were visualized by enzyme-linked chemiluminescence with an ECL kit. The primary antibodies were as follows: anti-MELK (ab108529), anti-α-tubulin (ab7291), and anti-mTOR (ab2732) from Abcam (Cambridge, UK); anti-4E-BP1 (#9644), anti-p-4E-BP1 (T37/46) (#2855), anti-S6 (#2317), anti-p-S6 (S235/236) (#4858), anti-p-PRAS40 (Thr246) (#13175), anti-p-PRAS40 (Ser183) (#5936), and

anti-raptor (#2280) from Cell Signaling Technology (Danvers, MA, USA); and anti-Flag from Sigma (#3165, St Louis, MO, USA). The immune complex was detected using HRP-conjugated secondary antibodies (ZSGB-BIO, Beijing, China). Rapamycin was purchased from Sigma (Solon, OH, USA).

Statistical Analysis

Data were analyzed using SPSS 16.0 (IBM, Armonk, NY, USA) or GraphPad Prism 5 (GraphPad, CA, USA). Groups from TCGA were compared by using an unpaired, two-tailed t-test or ANOVA and results were presented as mean $\pm$ SD. Kaplan–Meier curves and log-rank test were used to analyze the overall survival and disease-free survival of patients with ccRCC. Results from cell culture were analyzed by using an unpaired, two-tailed t-test and results are presented as mean $\pm$ SD. A p-value <0.05 was considered statistically significant and all experiments were repeated at least three times.

Results

Identification and Bioinformatics Analysis of the DEGs

To explore the DEGs between stage IV and stage I ccRCC, we first analyzed two independent RNA-seq data (TCGA, GSE73731). The preliminary analysis showed that a total of 1716 and 861 DEGs were extracted from TCGA and GSE73731 based on the R analysis and GEO2 (Fig. 1A). There were 86 common DEGs in both datasets (Fig. 1B), including 72 upregulated genes and 14 downregulated genes in stage IV ccRCC tissues compared with stage I ccRCC tissues. Then, GO enrichment and KEGG pathway analysis of DEGs with DAVID online suggested that the common DEGs were mainly enriched in biological processes related to mitotic nuclear division, cell division, G2/M transition mitotic cell, and cellular component associated with mid-body, spindle, kinesin complex, and cell cycle pathway (Fig. 1C). We further analyzed all common DEGs by using the STRING online database and Cytoscape software. A confidence score ≥ 0.7 was set as the cutoff criterion. The results showed that a total of 39 DEGs out of the 86 common DEGs were screened into the DEGs PPI network complex (Fig. 1D). Finally, MELK was filtered out as the seed gene in the network (Fig. 1E). These results suggested that MELK may play an important role in the progression of ccRCC.

Upregulation of MELK was Correlated with ccRCC Progression

In order to determine whether upregulation of MELK is correlated with disease progression, we analyzed the relationship between MELK expression and TNM stages of ccRCC patients in the TCGA database. The results suggested that MELK expression increased in patients with advanced ccRCC and was positively correlated with TNM stages (Fig. 2A). We subsequently evaluated the prognostic
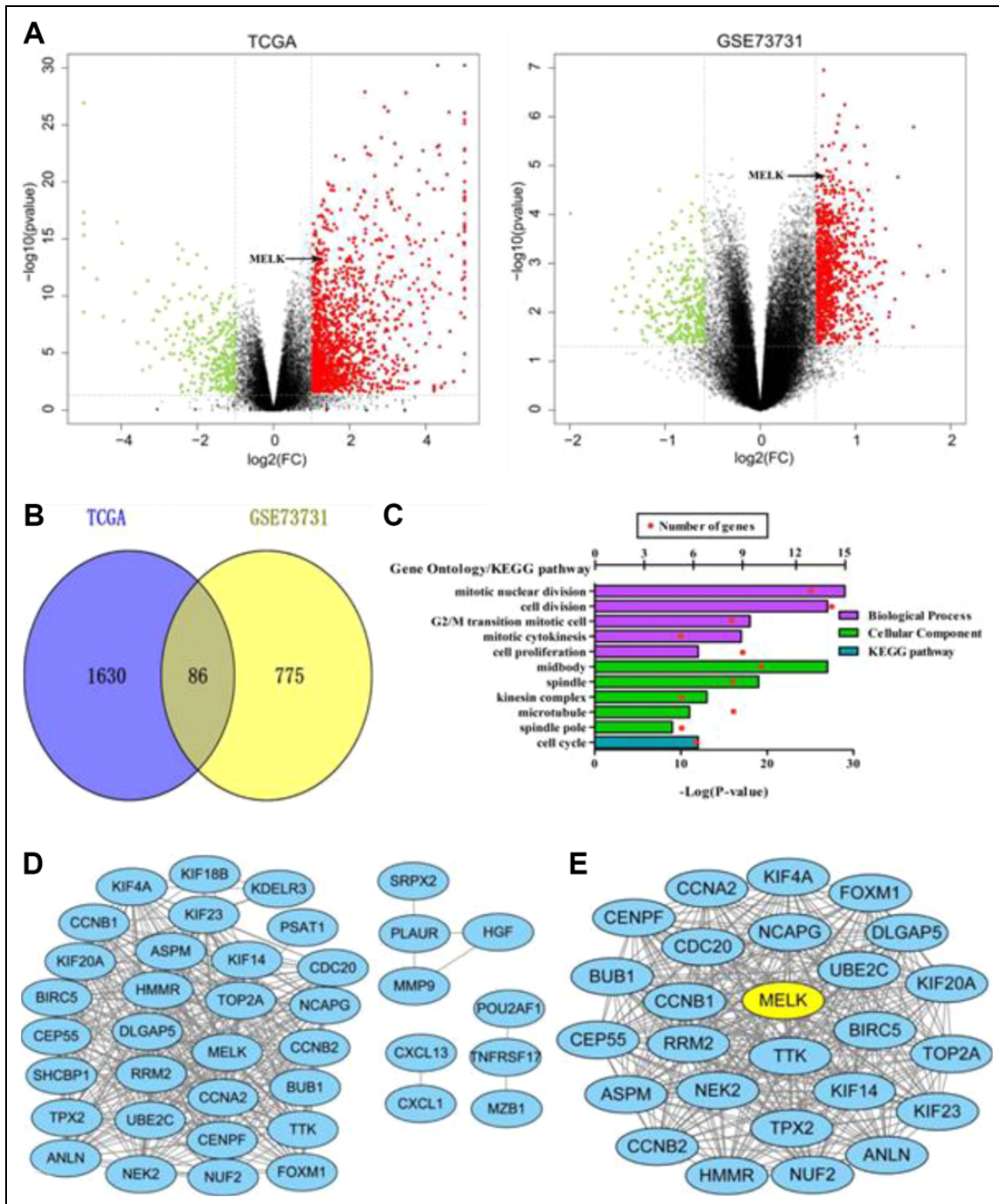
Figure 1. Differentially expressed genes (DEGs) screening and bioinformatics analysis. (A) Volcano plot showing relationship between magnitude of gene expression change (log2 of fold change; x-axis) and statistical significance of this change [–log10 of *p*-value; y-axis] in a comparison of stage IV and stage I ccRCC sample in TCGA and GSE73731 dataset. Red dots represent upregulated genes and green dots represent downregulated genes in stage IV compared with stage I ccRCC. (B) Identification of common DEGs in both TCGA and GSE73731. (C) The significant GO enrichment terms and KEGG enrichment pathway of common DEGs. Red dot means number of genes; bar chart means the –log (*p*-value) of the GO term and KEGG pathway. (D) DEGs protein–protein interaction (PPI) network containing 39 nodes and 352 edges. (E) One significant module composed of 26 nodes and 323 edges; yellow node represent seed gene in the module. Lines represent the interaction between nodes.

significance of MELK in these ccRCC patients. As shown in Fig. 2B, ccRCC patients with higher MELK expression (the median MELK expression value was used as the cutoff for low and high expression) had lower overall survival and disease-free survival rates than those with lower MELK expression. Taken together, these findings indicated that
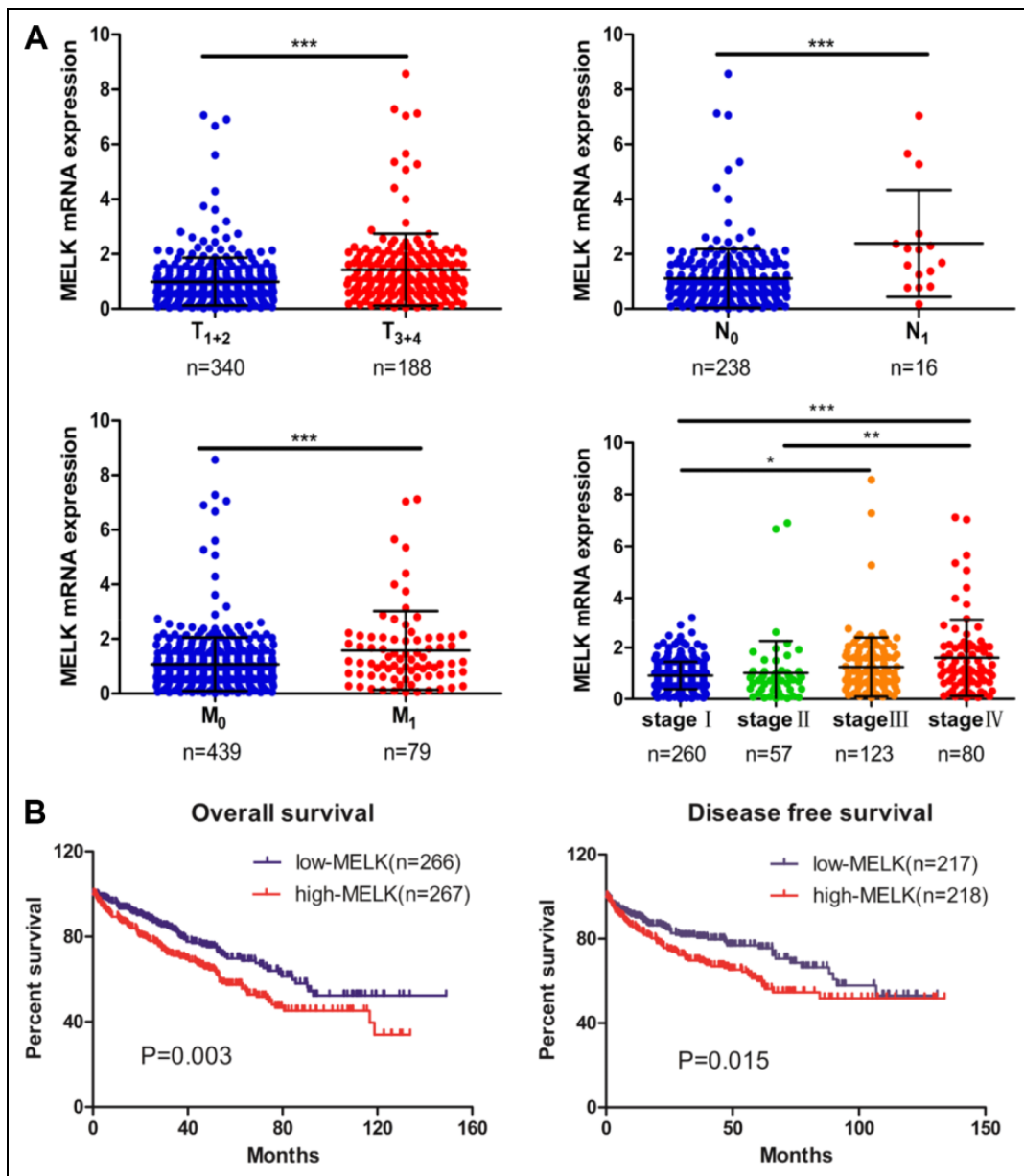
Figure 2. MELK was upregulated in advanced tumor stage and poor prognosis of patients with ccRCC. (A) Scatter diagram of relative MELK expression in different stages, with the horizontal lines representing the median, the vertical bars representing the standard deviation of data. Data were analyzed by two-tailed unpaired student's *t*-test or one-way ANOVA. (B) Kaplan–Meier survival curves of patients with ccRCC stratified by MELK expression levels, where the left one was based on overall survival time and the right one was based on disease-free survival time.*$p < 0.05$, **$p < 0.01$, ***$p < 0.001$.

upregulation of MELK may serve as an indicator in predicting poor prognosis of ccRCC and ccRCC progression.

Over-expression or Knock-down of MELK Promoted or Inhibited Proliferation, Invasion, and Colony Formation of ccRCC Cells

To investigate the role of MELK in ccRCC progression, we first determined the protein expression of MELK in ccRCC cell lines of ACHN and 769-P. As expected, MELK expression was relatively higher in ACHN cells isolated from metastatic foci than in 769-P cell lines isolated from primary foci (Fig. 3A). Then, in order to conduct gain-of-function and loss-of-function analysis, 769-P cells were transfected with MELK over-expression plasmids, whereas ACHN cells were transfected with MELK shRNA plasmids. The successful over-expression and knock-down of MELK models were confirmed by western blot (Fig. 3A and Fig. 3B). Subsequently, we employed these cell lines to perform biological function assays. The CCK-8 assay found that the
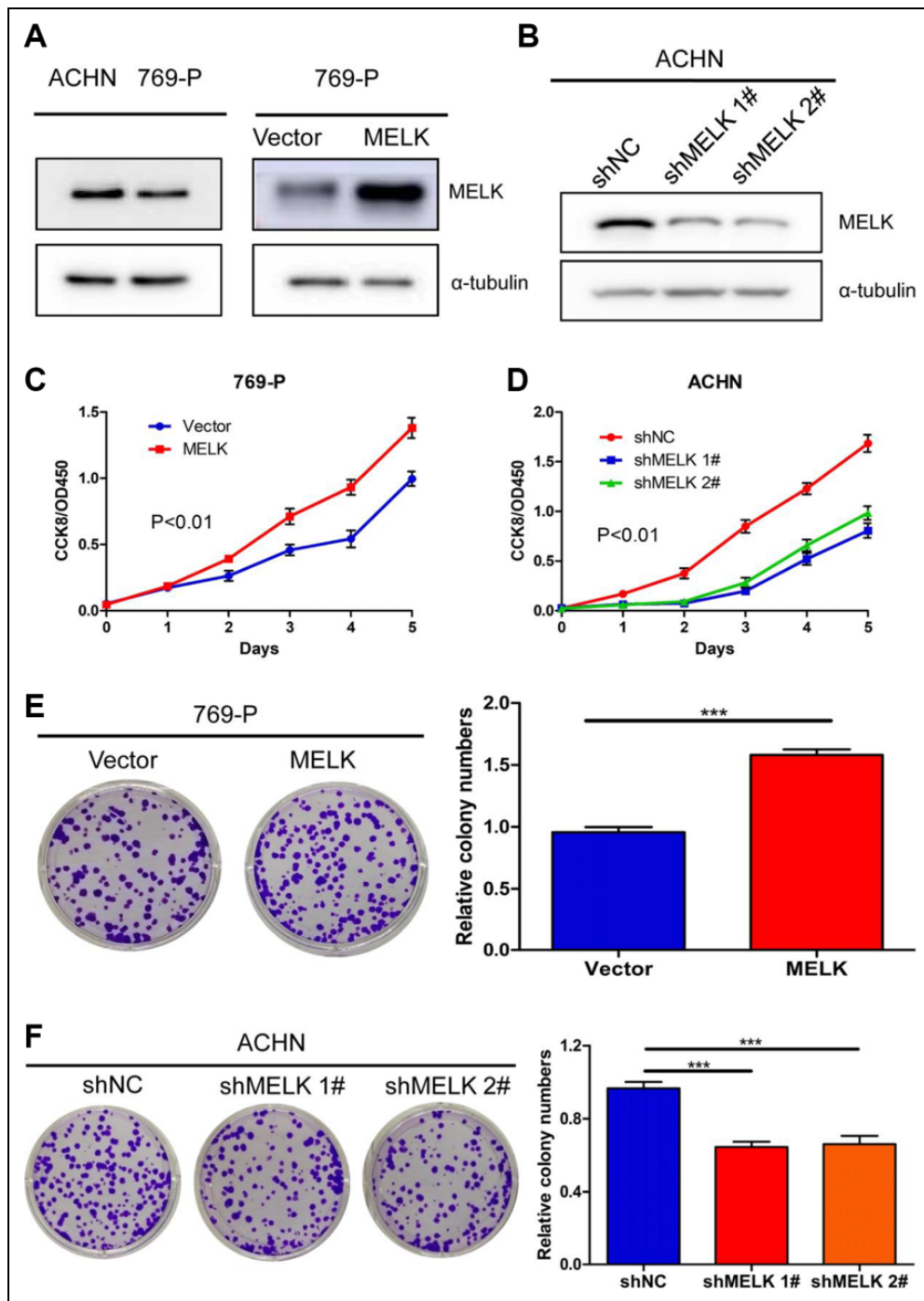
Figure 3. MELK promoted the malignant behaviors of ccRCC cells. (A) The expression levels of MELK in ACHN and 769-P cells were detected by western blot. 769-P cells were transfected with MELK plasmid or mock control, and successful over-expression of MELK was identified by western blot. (B) MELK knock-down by stable transfection of shRNA in ACHN cells were identified by western blotting. (C, D) The proliferation ability of 769-P cells over-expressing MELK, ACHN cells knocking-down MELK, and control cells was measured by CCK-8 assay. (E, F) The number of colonies of 769-P cells over-expressing MELK, ACHN cells knocking-down MELK, and control cells was measured by plate colony formation assay. (G, H) Migration and invasive capacity of 769-P cells over-expressing MELK and vector was measured by wound healing and transwell assay, respectively. (I, J) Migration and invasive capacity of ACHN cells knocking-down MELK and shNC was measured by wound healing and transwell assay, respectively. (K, L) The level of cyclin D1, cyclin A, N-Cadherin, Vimentin, and E-Cadherin of 769-P cells over-expressing MELK, ACHN cells knocking-down MELK, and control cells were detected. The data shown in the figures are representative data from at least three independent experiments. ***p<0.001.
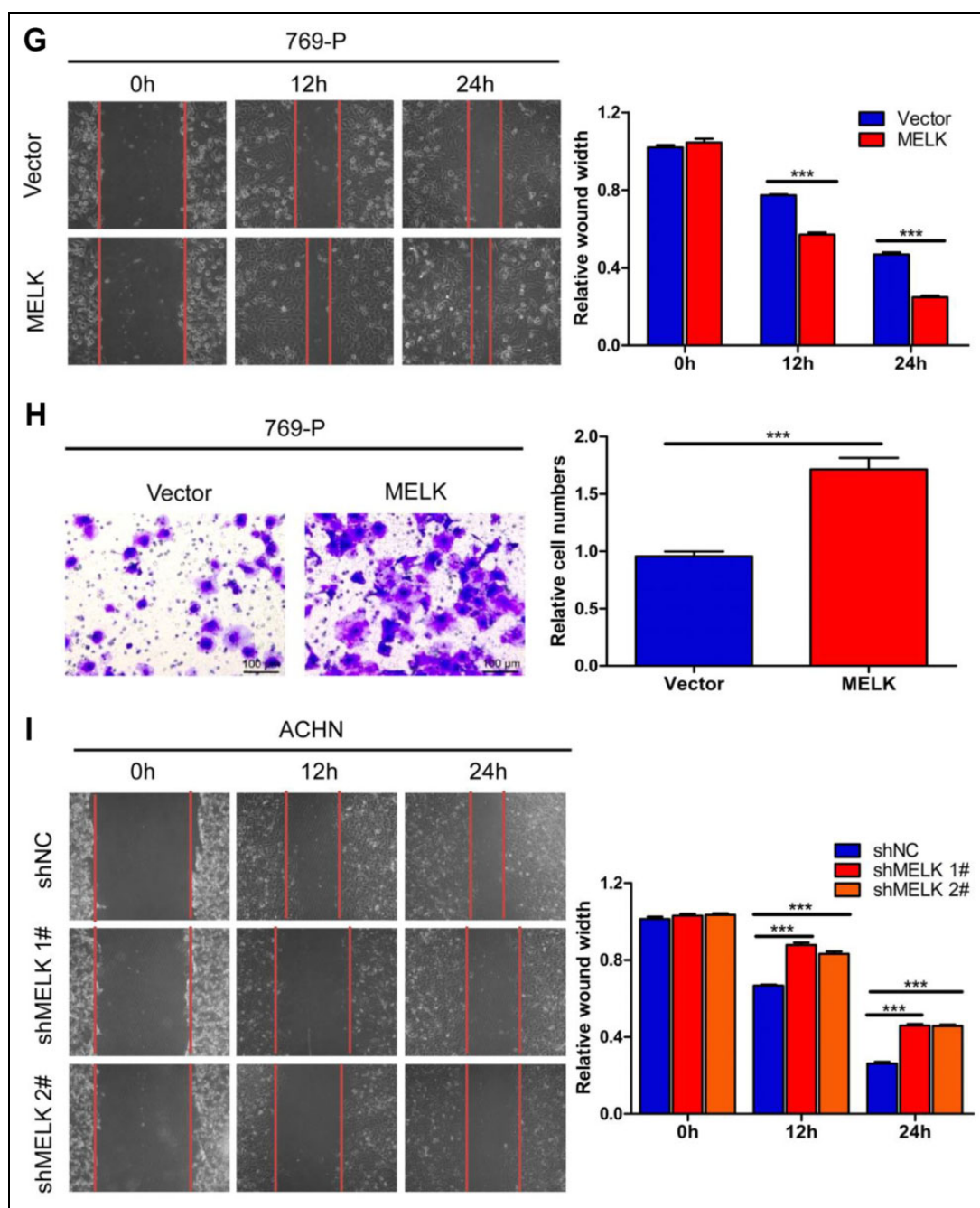
Figure 3. (Continued).

over-expression of MELK in 769-P cells significantly increased the viability (Fig. 3C), whereas knock-down of MELK in ACHN cells significantly reduced the viability (Fig. 3D). The promotive or prohibitive effects of MELK on the proliferation of ccRCC cells were further confirmed by the plate colony formation assay. As shown in Fig. 3E, the number of colonies markedly increased in 769-P cells over-expressing MELK, compared with the control group. On the contrary, ACHN cells knocking-down MELK formed fewer colonies than shNC control cells (Fig. 3F). Moreover, we

verified the effect of MELK on the migration and invasive capacity of 769-P and ACHN cells. The wound healing and transwell assay results showed that MELK over-expression significantly enhanced the migration (Fig. 3G) and invasive (Fig. 3H) potential of 769-P cells. Knock-down of MELK in ACHN cells significantly inhibited migration (Fig. 3I) and invasive (Fig. 3J) capacity compared with shNC control cells. Consistent with these results, over-expression of MELK increased levels of cyclin D1, cyclin A, N-Cadherin, and Vimentin, and reduced levels of E-Cadherin compared with
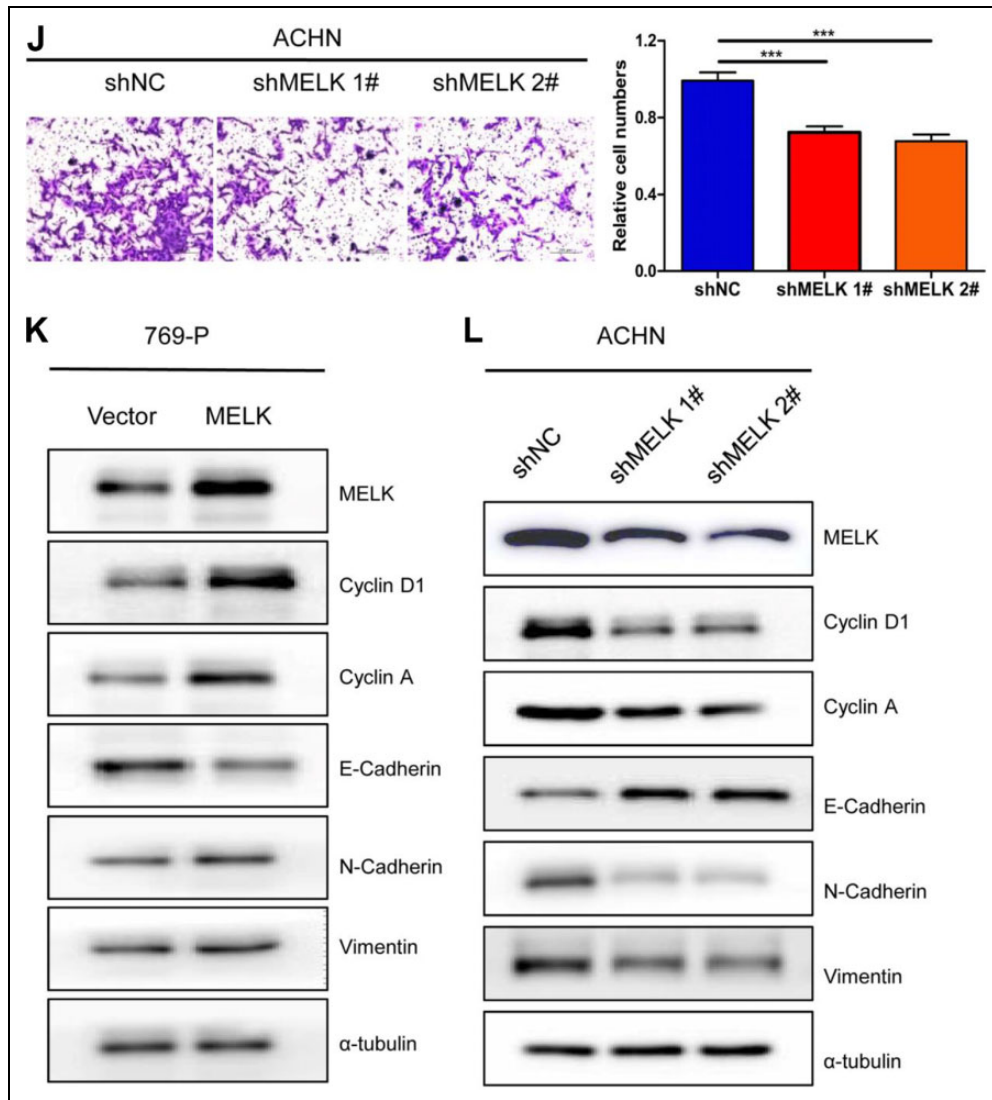
Figure 3. (Continued).

vector control cells (Fig. 3K), whereas knock-down of MELK reduced levels of cyclin D1, cyclin A, N-Cadherin, and Vimentin, and increased levels of E-Cadherin compared with shNC control cells (Fig. 3L). Added up, these findings suggested that MELK promoted the progression of ccRCC.

MELK Promoted the Progression of ccRCC by Activating mTORC1 Pathway

To investigate the effect of MELK on ccRCC progression, we conducted Gene Set Enrichment Analysis (GSEA) for MELK with higher and lower expression. The results showed that in both TCGA and GSE73731 databases (Fig. 4A), the mTORC1 pathway was upregulated in the higher expression MELK group. Previous studies have reported that mTORC1 pathway plays an important role in the progression

of various tumors. We thus hypothesized that MELK might promote ccRCC progression by activating the mTORC1 pathway. We first determined whether MELK could regulate the mTORC1 pathway by using western blot analysis. Results showed that over-expression of MELK in 769-P cells significantly activated the mTORC1 pathway as evaluated by its downstream signaling molecules, including S6K1 and 4E-BP1. In addition, the increase in the ratio of phosphorylated S6K1 to S6K1 further confirmed the activation of the mTORC1 pathway (Fig. 4B and Fig. 4C). Conversely, knock-down of MELK in ACHN cells inhibited the activity of the mTORC1 pathway (Fig. 4D and Fig. 4E). Given that MELK can promote the progression of ccRCC and activate the mTORC1 pathway, it is reasonable to assume that activation of the mTORC1 pathway mediates the function of MELK. As shown in Fig. 4F, the rise in P-S6K1 and P-4EBP1 and the increase in the ratio of P-S6K1 to S6K1
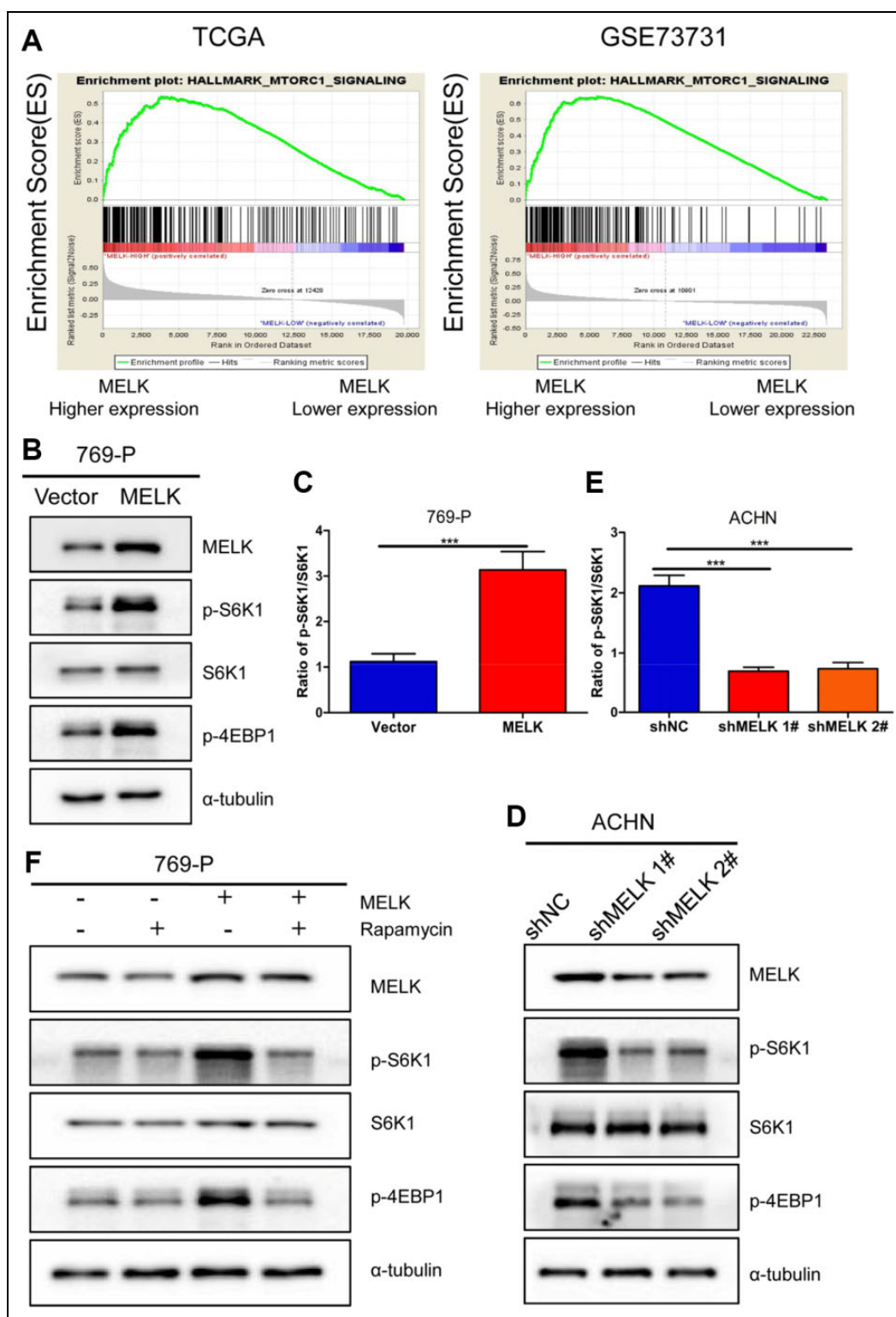
Figure 4. MELK promoted activation of mTORC1. (A) Enrichment plots of gene expression signatures for mTORC1pathway activation according to MELK mRNA expression levels by GSEA of TCGA and GSE73731 ccRCC database. The samples were divided into high and low MELK expression groups based on the median values of MELK RNA-seq quantification results. The results showed that MELK level had significant positive correlation with mTORC1 activation in ccRCC samples. $p<0.05$ and FDR <0.25 was considered as statistically significant. (B) 769-P cells transfected with MELK plasmid or mock control were cultured for 48 h before western blot assay for mTORC1 pathway activity. (C) After transfection with MELK, the ratio of the phosphorylated form of S6K1 to its total form was further analyzed. (D) ACHN cells transfected with shMELK or shControl were cultured for 48 h before western blot assay. (E) After transfection with shMELK, the ratio of the phosphorylated form of S6K1 to its total form was further analyzed. (F) 769-P cells transfected with MELK plasmid were treated with rapamycin (100 nM) for 24 h. Inhibition of the mTORC1 pathway was analyzed by western blot.***$p<0.001$.

mediated by MELK were significantly eliminated when we blocked the mTORC1 pathway with 100 nM rapamycin, a specific mTOR inhibitor. Together, these results suggested that over-activation of the mTORC1 pathway was responsible for the MELK-mediated malignant phenotype of ccRCC cells.

MELK Involvement in mTROC1 Pathway by Phosphorylating PRAS40

Previous studies have found that proline-rich Akt substrate 40 (PRAS40) inhibits activation of the mTORC1 pathway and Akt-mediated phosphorylation of PRAS40 prevents its inhibition of mTORC1[17]. PRAS40 inhibits mTORC1 through competing with other substrates for raptor[17–19]. The dissociation of PRAS40 from raptor requires phosphorylation of PRAS40 at some sites[20]. Therefore, we examined whether MELK could regulate mTROC1 activation by phosphorylating PRAS40. We initially used western blot to evaluate levels of phosphorylating PRAS40, mTOR, and raptor in 769-P cells over-expressing MELK and ACHN cells knocking-down MELK. The results showed that over-expression of MELK in 769-P cells significantly increased p-PRAS40 (T246), whereas knock-down of MELK in ACHN cells had the opposite effect (Fig. 5A and Fig. 5B). In addition, over-expressing or knock-down of MELK had no effect on levels of mTOR, raptor, and p-PRAS40 (S183). Then, to verify the interaction between PRAS40 and raptor in ccRCC cells, we transiently transfected Flag-PRAS40 into 769-P and ACHN cells and performed coimmunoprecipitation assays. As shown in Fig. 5C and Fig. 5D, raptor was pulled down by exogenous Flag-PRAS40, indicating that raptor and PRAS40 co-exist in a protein complex. Finally, we investigated whether the phosphorylation of PRAS40 (T246) by MELK is sufficient to release PRAS40 from raptor. We over-expressed Flag-PRAS40 in the constructed cell models and detected whether there existed changes in the interaction between raptor and PRAS40. Coimmunoprecipitation assays indicated that raptor increased in PRAS40 immunoprecipitates in knock-down of MELK ACHN cells (Fig. 5E). Inversely, over-expression of MELK significantly inhibited the interaction between PRAS40 and raptor in 769-P cells (Fig. 5F). Taken together, these findings suggested that MELK phosphorylates PRAS40 at T246 and enhances mTORC1 activity by dissociating PRAS40 from raptor.

Discussion

ccRCC is the most common type of renal cell carcinoma, and patients with advanced stage disease generally have poor prognosis. Elucidating the mechanism of ccRCC progression and finding new therapeutic targets have both theoretical and clinical implications. In our study, DEGs between stage IV and stage I ccRCC were initially screened by comparing the RNA-seq data from TCGA and GSE73731 databases. Next,

GO enrichment and KEGG pathway analysis indicated that DEGs were enriched in mitotic division and cell cycle. Furthermore, *MELK*, the seed gene in the module, was screened out after PPI network construction and module analysis.

MELK is a member of the snf1/AMPK family of protein serine/threonine kinases[21,22] which is critical for a range of biological functions, including mitotic progression, proliferation, apoptosis, and tumorigenesis[23–26]. So far, significantly higher levels of MELK have been reported in human cancers of the breast, colon, pancreas, brain, and prostate compared with normal cells[27]. Moreover, previous studies have found the correlation between MELK expression and tumor progression for breast cancer and astrocytoma as well as prostate cancer[28–31]. Over-expression of MELK has also been found to be correlated with poor survival in multiple cancer types[31–33]. Consistent with these findings, our results showed that MELK is upregulated in stage IV ccRCC tissues compared with stage I counterparts, and that over-expression of MELK is significantly correlated with both adverse clinicopathological characteristics and poor prognosis. Subsequently, to explore the function of MELK in ccRCC, we performed gain-of-function and loss-of-function analyses and found that MELK promotes ccRCC cell proliferation, colony formation, invasion, and migration. These findings suggested that MELK has a promotive effect in the progression of ccRCC.

Previous studies have reported that MELK may play a key role in tumor progression in various cancers through FOXM1 signaling[26], eIF4B signaling[34], and the NF-κB pathway[35]. Interestingly, using GSEA assay[36], our signaling pathway screening showed that the mTORC1 pathway is enriched in the MELK higher expression group compared with the MELK lower counterparts. Given the importance of mTOR activation and targeting in poor prognosis ccRCC[37,38], we hypothesized that MELK might promote ccRCC progression by activating the mTORC1pathway. As expected, our results showed that MELK over-expression significantly activated the mTORC1 pathway, whereas knock-down of MELK did not. Moreover, inhibiting mTOR activity by rapamycin could significantly suppress mTORC1 activation in MELK-upregulated ccRCC cells. These findings indicated that MELK may act as an upstream molecule of mTOR and therefore has a regulatory effect. Further investigation showed that MELK promotes mTORC1 pathway activity through phosphorylating PRAS40, an inhibitory subunit of the mTORC1 pathway[39,40]. Previous studies have suggested that PRAS40 inhibits mTORC1 activity through competing with substrates for raptor[19]. Phosphorylation of PRAS40 releases PRAS40 from mTORC1 allowing increased activity[41], although there is little consensus about the phosphorylation sites. Rho et al. reported that phosphorylation at Thr246 is sufficient to release PRAS40 from mTORC1, both *in vitro* and *in vivo*[41,42]. Wang et al. found that dissociation of PRAS40
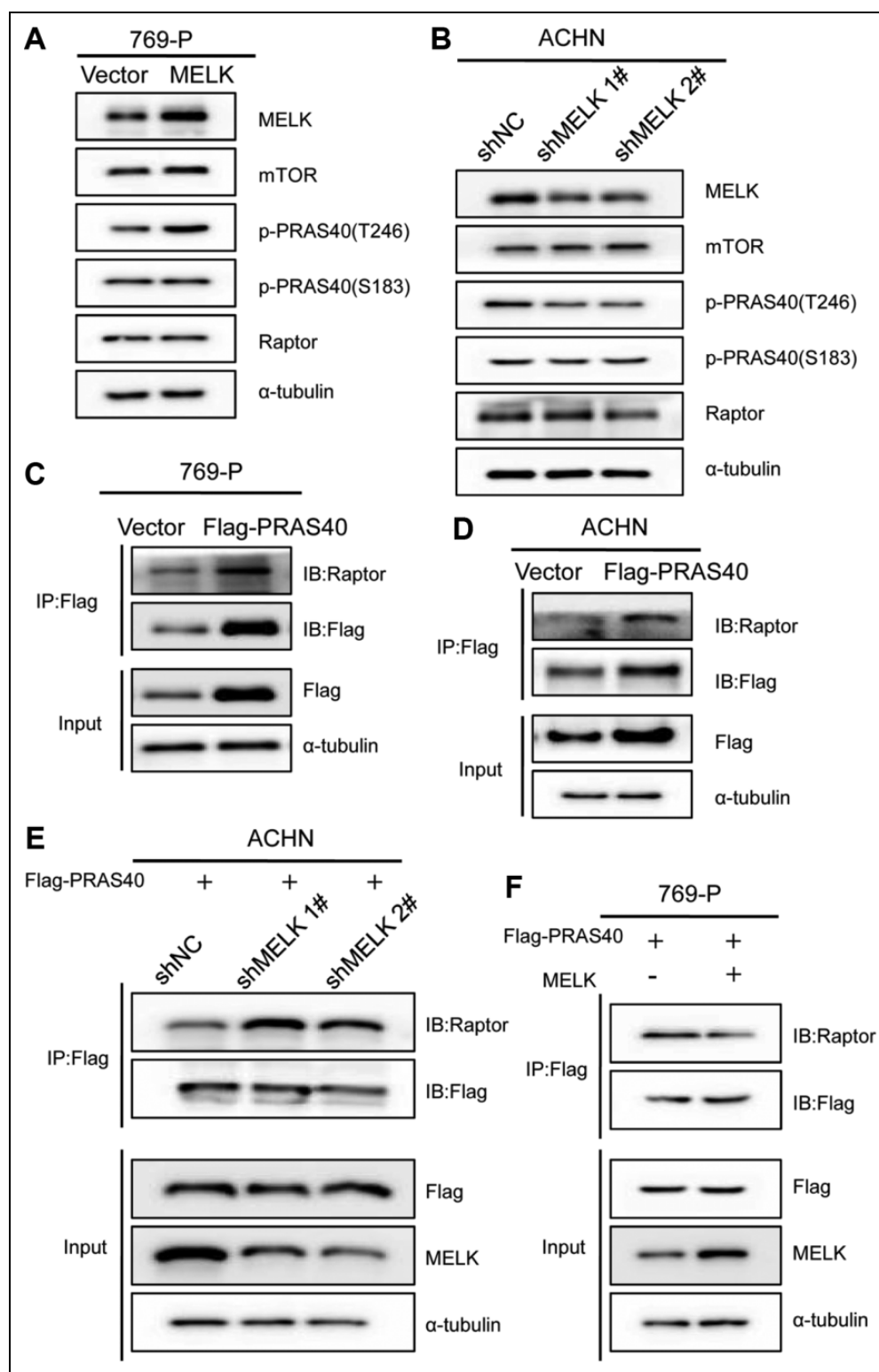
Figure 5. Over-expression of MELK promoted PRAS40 phosphorylation at Thr 246 and released PRAS40 from the raptor. (A) After 48 h transfection with constructs of MELK or control vectors in 769-Pcells, the main components of mTORC1 and its regulatory molecules were detected by western blot. (B) ACHN cells were transfected with lentiviral packaged with shMELK or shControl for 48 h, the main components of mTORC1 and its regulatory molecules were detected by western blot. (C, D) 769-P and ACHN cells transfected with Flag-PRAS40 plasmid or control vector were analyzed with coimmunoprecipitation using anti-Flag from whole cell lysates. Protein levels of PRAS40 and raptor were detected. (E) ACHN cells transfected with shMELK or shControll were over-expressed Flag-PRAS40 and analyzed with coimmunoprecipitation using anti-Flag antibody from whole cell lysates. (F) 769-P cells transfected with MELK plasmid or control vector were over-expressed Flag-PRAS40 and analyzed with coimmunoprecipitation using anti-Flag antibody from whole cell lysates. The cell lysates and immunoprecipitates were subjected to western blot analysis using the indicated antibodies.

from mTORC1 requires simultaneous phosphorylation of PRAS40 on T246 by Akt, and on S183 by mTOR itself[43,44]. In our study, we observed that over-expression of MELK only increased the PRAS40 phosphorylation at Thr246, not at S183. Knock-down of MELK decreased the PRAS40 phosphorylation at Thr246 and had no effect on S183. More importantly, we confirmed that over-expression of MELK— that is, phosphorylating PRAS40 at Thr246—could disrupt the interaction between PRAS40 and raptor whereas knock-down of MELK could not.

Combining bioinformatics analysis and experiments, our research suggests that MELK may play a crucial role in the progression of ccRCC. Phosphorylation of PRAS40 at Thr246 by MELK dissociates PRAS40 from raptor and also augments mTORC1 pathway activity. Together, MELK represents a promising molecular and for future studies on mTORC1 signaling in ccRCC progression.

Ethical Approval

The study protocol was approved by the Luoyang Central Hospital Medical Ethics Committee(#01/03/18).

Statement of Human and Animal Rights

All procedures in this study were conducted in accordance with the study protocol approved by Luoyang Central Hospital Medical Ethics Committee (#01/03/18).

Statement of Informed Consent

Written informed consent was obtained from the patients for their anonymized information to be published in this article.

Declaration of Conflicting Interests

The author(s) declared no potential conflicts of interest with respect to the research, authorship, and/or publication of this article.

Funding

ORCID iD

Han Zhang ![ORCID] https://orcid.org/0000-0002-9101-4170

Supplemental Material

Supplemental material for this article is available online.

Notes

1. The Cancer Genome Atlas: https://cancergenome.nih.gov/
2. Relevant data can be found at: http://www.ncbi.nlm.nih.gov/geo
3. Relevant data can be found at: http://string-db.org/
4. http://software.broadinstitute.org-/gsea/msigdb

References

1. Bray F, Ferlay J, Soerjomataram I, Siegel RL, Torre LA, Jemal A. Global cancer statistics 2018: GLOBOCAN estimates of incidence and mortality worldwide for 36 cancers in 185 countries. CA Cancer J Clin. 2018;68(6):394–424. [Epub 2018 Sep 12]

2. Herman JG, Latif F, Weng Y, Lerman MI, Zbar B, Liu S, Samid D, Duan DS, Gnarra JR, Linehan WM. Silencing of the VHL tumor-suppressor gene by DNA methylation in renal carcinoma. Proc Natl Acad Sci U S A. 1994;91(21): 9700–9704.

3. Kaelin WG, Ratcliffe PJ. Oxygen sensing by metazoans: the central role of the HIF hydroxylase pathway. Mol Cell. 2008; 30(4):393–402.

4. Eisen T, Gossage L. Alterations in VHL as potential biomarkers in renal-cell carcinoma. Nat Rev Clin Oncol. 2010;7(5): 277–288.

5. Bertout JA, Majmundar AJ, Gordan JD, Lam JC, Ditsworth D, Keith B, Brown EJ, Nathanson KL, Simon MC. HIF2α inhibition promotes p53 pathway activity, tumor cell death, and radiation responses. Proc Natl Acad Sci U S A. 2009; 106(34):14391–6.

6. Gordan JD, Bertout JA, Hu C, Diehl JA, Simon MC. HIF-2α promotes hypoxic cell proliferation by enhancing c-Myc transcriptional activity. Cancer Cell. 2007;11(4):335–347.

7. Peña-Llopis S, Vega-Rubín-de-Celis S, Liao A, Leng N, Pavía-Jiménez A, Wang S, Yamasaki T, Zhrebker L, Sivanand S, Spence P, Kinch L, et al. BAP1 loss defines a new class of renal cell carcinoma. Nat Genet. 2012;44(7):751–759.

8. Miao D, Margolis CA, Gao W, Voss MH, Li W, Martini DJ, Norton C, Bossé D, Wankowicz SM, Cullen D, Horak C, et al. Genomic correlates of response to immune checkpoint therapies in clear cell renal cell carcinoma. Science. 2018; 359: 801–806.

9. Hakimi AA, Chen Y, Wren J, Gonen M, Abdel-Wahab O, Heguy A, Liu H, Takeda S, Tickoo SK, Reuter VE, Voss MH, et al. Clinical and pathologic impact of select chromatin-modulating tumor suppressors in clear cell renal cell carcinoma. Eur Urol. 2013;63(5):848–854.

10. Ho TH, Serie DJ, Parasramka M, Cheville JC, Bot BM, Tan W, Wang L, Joseph RW, Hilton T, Leibovich BC, Parker AS, et al. Differential gene expression profiling of matched primary renal cell carcinoma and metastases reveals upregulation of extracellular matrix genes. Ann Oncol. 2017;28(3):604–610.

11. Gentleman RC, Carey VJ, Bates DM, Bolstad B, Dettling M, Dudoit S, Ellis B, Gautier L, Ge Y, Gentry J, Hornik K, et al. Bioconductor: open software development for computational biology and bioinformatics. Genome Biol. 2004;5(10):R80. 1-R80.16.

12. Barrett T, Wilhite SE, Ledoux P, Evangelista C, Kim IF, Tomashevsky M, Marshall KA, Phillippy KH, Sherman PM, Holko M, Yefanov A, et al. NCBI GEO: archive for functional genomics data sets—update. Nucleic Acids Res. 2012;41: D991–D995.

13. Huang DW, Sherman BT, Lempicki RA. Systematic and integrative analysis of large gene lists using DAVID bioinformatics resources. Nat Protoc. 2009;4(1):44–57.

14. Huang DW, Sherman BT, Lempicki RA. Bioinformatics enrichment tools: paths toward the comprehensive functional

analysis of large gene lists. Nucleic Acids Res. 2009;37(1): 1–13.

15. Szklarczyk D, Morris JH, Cook H, Kuhn M, Wyder S, Simonovic M, Santos A, Doncheva NT, Roth A, Bork P, Jensen LJ, et al. The STRING database in 2017: quality-controlled protein–protein association networks, made broadly accessible. Nucleic Acids Res. 2017;45(D1):D362–D368.

16. Bader GD, Hogue CWV. An automated method for finding molecular complexes in large protein interaction networks. BMC Bioinformatics. 2003;4:2.

17. Sancak Y, Thoreen CC, Peterson TR, Lindquist RA, Kang SA, Spooner E, Carr SA, Sabatini DM. PRAS40 is an insulin-regulated inhibitor of the mTORC1 protein kinase. Mol Cell. 2007;25(6): 903–915.

18. Dibble CC, Cantley LC. Regulation of mTORC1 by PI3 K signaling. Trends Cell Biol. 2015;25(9):545–555.

19. Wang L, Harris TE, Roth RA, Lawrence JC. PRAS40 regulates mTORC1 kinase activity by functioning as a direct inhibitor of substrate binding. J Biol Chem. 2007;282(27):20036–20044.

20. Wang L, Harris TE, Lawrence JC. Regulation of Proline-rich Akt Substrate of 40 kDa (PRAS40) function by mammalian target of rapamycin complex 1 (mTORC1)-mediated phosphorylation. J Biol Chem. 2008;283(23):15619–15627.

21. Gil M, Yang Y, Lee Y, Choi I, Ha H. Cloning and expression of a cDNA encoding a novel protein serine/threonine kinase predominantly expressed in hematopoietic cells. Gene. 1997; 195(2):295–301.

22. Heyer BS, Warsowe J, Solter D, Knowles BB, Ackerman SL. New member of the Snf1/AMPK kinase family, Melk, is expressed in the mouse egg and preimplantation embryo. Mol Reprod Dev. 1997;47(2):148–156.

23. Pickard MR, Mourtada-Maarabouni M, Williams GT. Candidate tumour suppressor Fau regulates apoptosis in human cells: an essential role for Bcl-G. Biochim Biophys Acta. 2011; 1812(9):1146–1153.

24. Blot J, Chartrain I, Roghi C, Philippe M, Tassan J. Cell cycle regulation of pEg3, a new xenopus protein kinase of the KIN1/ PAR-1/MARK family. Dev Biol. 2002;241(2):327–338.

25. Lin ML, Park JH, Nishidate T, Nakamura Y, Katagiri T. Involvement of maternal embryonic leucine zipper kinase (MELK) in mammary carcinogenesis through interaction with Bcl-G, a pro-apoptotic member of the Bcl-2 family. Breast Cancer Res. 2007;9(1):R17.

26. Joshi K, Banasavadi-Siddegowda Y, Mo X, Kim S, Mao P, Kig C, Nardini D, Sobol RW, Chow LML, Kornblum HI, Waclaw R, et al. MELK-dependent FOXM1 phosphorylation is essential for proliferation of glioma stem cells. Stem Cells. 2013; 31(6):1051–1063.

27. Gray D, Jubb AM, Hogue D, Dowd P, Kljavin N, Yi S, Bai W, Frantz G, Zhang Z, Koeppen H, de Sauvage FJ, et al. Maternal embryonic leucine zipper kinase/murine protein serine-threonine kinase 38 is a promising therapeutic target for multiple cancers. Cancer Res. 2005;65(21):9751–9761.

28. Pickard M, Green A, Ellis I, Caldas C, Hedge V, Mourtada-Maarabouni M, Williams G. Dysregulated expression of Fau and MELK is associated with poor prognosis in breast cancer. Breast Cancer Res. 2009;11(4):R60.

29. Marie SKN, Okamoto OK, Uno M, Hasegawa APG, Oba-Shinjo SM, Cohen T, Camargo AA, Kosoy A, Carlotti CG, Toledo S, Moreira-Filho CA, et al. Maternal embryonic leucine zipper kinase transcript abundance correlates with malignancy grade in human astrocytomas. Int J Cancer. 2008;122(4): 807–815.

30. Kuner R, Fälth M, Pressinotti NC, Brase JC, Puig SB, Metzger J, Gade S, Schäfer G, Bartsch G, Steiner E, Klocker H, et al. The maternal embryonic leucine zipper kinase (MELK) is upregulated in high-grade prostate cancer. J Mol Med. 2013;91(2):237–248.

31. Jurmeister S, Ramos-Montoya A, Sandi C, Pertega-Gomes N, Wadhwa K, Lamb AD, Dunning MJ, Attig J, Carroll JS, Fryer LG, Felisbino SL, et al. Identification of potential therapeutic targets in prostate cancer through a cross-species approach. Embo Mol Med. 2018;10(3):e8274.

32. Li Y, Tang H, Sun Z, Bungum AO, Edell ES, Lingle WL, Stoddard SM, Zhang M, Jen J, Yang P, Wang L. Network-based approach identified cell cycle genes as predictor of overall survival in lung adenocarcinoma patients. Lung Cancer. 2013;80(1):91–98.

33. Choi S, Ku J. Resistance of colorectal cancer cells to radiation and 5-FU is associated with MELK expression. Biochem Biophys Res Commun. 2011;412(2):207–213.

34. Wang Y, Begley M, Li Q, Huang H, Lako A, Eck MJ, Gray NS, Mitchison TJ, Cantley LC, Zhao JJ. Mitotic MELK-eIF4B signaling controls protein synthesis and tumor cell survival. Proc Natl Acad Sci U S A. 2016;113(35):9810–9815.

35. Janostiak R, Rauniyar N, Lam TT, Ou J, Zhu LJ, Green MR, Wajapeyee N. MELK promotes melanoma growth by stimulating the NF-κB pathway. Cell Rep. 2017;21(10): 2829–2841.

36. Subramanian A, Tamayo P, Mootha VK, Mukherjee S, Ebert BL, Gillette MA, Paulovich A, Pomeroy SL, Golub TR, Lander ES, Mesirov JP. Gene set enrichment analysis: a knowledge-based approach for interpreting genome-wide expression profiles. Proc Natl Acad Sci U S A. 2005; 102(43):15545–15550.

37. Shariat SF, Karam JA, Karakiewicz PI. Re: Temsirolimus, interferon alfa, or both for advanced renal-cell carcinoma. Eur Urol. 2009;55(1):250–252.

38. Capitanio U, Montorsi F. Renal cancer. Lancet. 2016; 387(10021):894–906.

39. Kovacina KS, Park GY, Bae SS, Guzzetta AW, Schaefer E, Birnbaum MJ, Roth RA. Identification of a proline-rich Akt substrate as a 14-3-3 binding partner. J Biol Chem. 2003; 278(12):10189–10194.

40. Haar EV, Lee S, Bandhakavi S, Griffin TJ, Kim D. Insulin signalling to mTOR mediated by the Akt/PKB substrate PRAS40. Nat Cell Biol. 2007;9(3):316–323.

41. Oshiro N, Takahashi R, Yoshino K, Tanimura K, Nakashima A, Eguchi S, Miyamoto T, Hara K, Takehana K, Avruch J, Kikkawa U, et al. The proline-rich Akt substrate of 40 kDa (PRAS40)

is a physiological substrate of mammalian target of rapamycin complex 1. J Biol Chem. 2007;282(28):20329–20339.

42. Rho O, Srivastava J, Cho J, DiGiovanni J. Overexpression of PRAS40T246A in the proliferative compartment suppresses mtorc1 signaling, keratinocyte migration, and skin tumor development. J Invest Dermatol. 2016;136(10):2070–2079.

43. Wang L, Harris TE, Lawrence JC. Regulation of proline-rich Akt substrate of 40 kDa (PRAS40) function by mammalian target of rapamycin complex 1 (mTORC1)-mediated phosphorylation. J Biol Chem. 2008;283(23): 15619–15627.

44. Rapley J, Oshiro N, Ortiz-Vega S, Avruch J. The mechanism of insulin-stimulated 4E-BP protein binding to mammalian target of rapamycin (mTOR) Complex 1 and its contribution to mTOR Complex 1 signaling. J Biol Chem. 2011;286(44): 38043–38053.